Understanding geothermal reservoirs using 3D modelling techniques: A case study of the Ebino prospect, Southern Japan

Elliot Humphrey[1], Hugh O'Keeffe[1], Jeremy O'Brien[2] and Hiromi Honda[3]

[1]Geothermal Development & Investment, 2-3-18 Shiba, Minato-ku, Shibakoen Building 3F, Tokyo, Japan.

[2]ARANZ Geo, 20 Moorhouse Ave, Addington, Christchurch 8011, New Zealand.

[3]The University of Tokyo, Kashiwa Campus, 5-1-5 Kashiwano-ha, Kashiwa-shi, Chiba 277-8561, Japan.

Elliot.humphrey@chinetsu.com, Hugh.okeeffe@chinetsu.com, Jeremy.obrien@aranzgeo.com, Hiromi.honda@chinetsu.com

Keywords: *Ebino, geothermal exploration, geological model, Leapfrog, Seismo-Electric, Japan*

ABSTRACT

Current success rates for geothermal exploration wells are approximately 50% (IFC, 2013) and whilst results have improved over time, this still poses a high risk for small scale geothermal development. This project integrates existing and recently acquired data to create 3D geological models which identify higher potential drilling targets and mitigate exploration-based risk.

The Ebino prospect, located in southern Japan, has been previously explored by the Japanese government in the early 1990`s where exploration data determined the area prospective for geothermal development. The survey area is situated on the northwest side of the Kirishima Volcanic Complex, segmented by two main valleys that straddle Quaternary-aged lava flows. Subsurface geology consists of sub-horizontal lava flows and pyroclastic deposits that have been partially fractured by NW-SE fault zones. Because of challenging topographic conditions, identifying an accessible wellsite for cost-effective drilling is necessary.

Seismo-Electric (SE) surveying (Skokan & Chi, 1993) was selected for its mobility in challenging topographies and ability to vertically detect fluids without the need for large horizontal areas compared with other surface geophysical methods. A static geological model was initially created using existing borehole and geophysical data. The models display geological geometries and structural variations, whilst borehole temperature data creates isotherms to characterize reservoir conditions. SE data later updated the original model to define the architecture of fluid-saturated fracture zones to improve well planning and design. The model allows visualization of subsurface geology and reservoir architecture, helping to identify higher potential drill targets. Geological modelling indicated that higher potential drill targets exist closer to fault zones in the southern part of the prospect area.

This project illustrates the effectiveness of a synthetic study of geological datasets that support decisions for geothermal well planning and design. Integrated geological modelling techniques can reduce exploration-based risk in decisions for geothermal development.

1. INTRODUCTION

The Ebino prospect is located on the northwestern flank of the Kirishima Volcanics, a NW-SE elongated area of Pleistocene to Holocene aged calderas, approximately 50 km northeast of Kagoshima in Southern Japan (Fig.1). The area has been of interest for geothermal development since the early 1990s, where previous exploration campaigns have confirmed the viability of geothermal power generation (NEDO, 1997). Because of this, SE geophysical surveying was recently conducted to better understand the distribution of fluid saturated zones in the subsurface.

This paper aims to investigate the geothermal potential of the Ebino area by integrating data from previous exploration with SE surveying using 3D modelling techniques. By doing so, this study aims to re-evaluate existing geological interpretations to ultimately reduce future risk during well planning and design. The focus of modelling is to improve reservoir characterisation within the Ebino area, rather than visualizing the entire geothermal system.

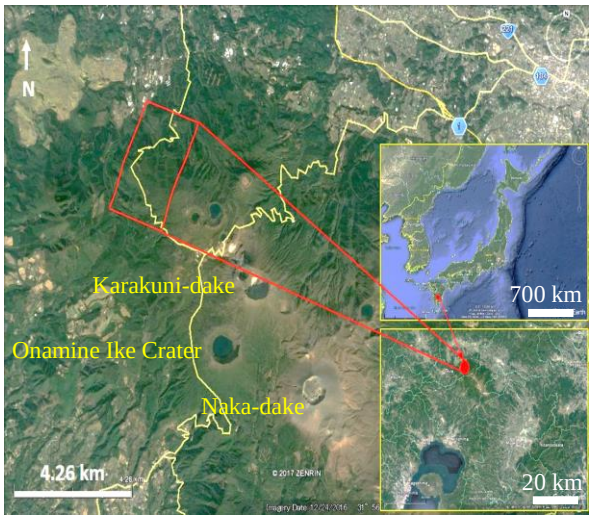

Figure 1: Location of Ebino and model area (Courtesy of Google Earth, 2017)

2. GEOLOGICAL SETTING

2.1 Tectonic setting

Tectonic activity in Southern Kyushu is associated with the subduction of the Philippines Sea Plate under the Eurasian plate along the Nankai Trough (Park *et al.*, 2009), with subduction occurring in two main pulses at 15Ma and 6Ma (Watanabe, 2005). The Philippines Sea Plate is divided by the Kyushu-Palau Ridge (KPR) which subducted in the Nankai Trough between 15-12Ma (Kimura, 1996) and progressively migrated to the northeast. B/Nb isotope ratios indicate the subduction of the KPR between 15-10Ma was responsible for volcanism in Southern Kyushu (Miyoshi *et al.*, 2008) with Shibata *et al.* (2014) suggesting that subducted margins of the KPR are responsible for separated volcanism at both Kirishima and Mt Aso (Fig 2).

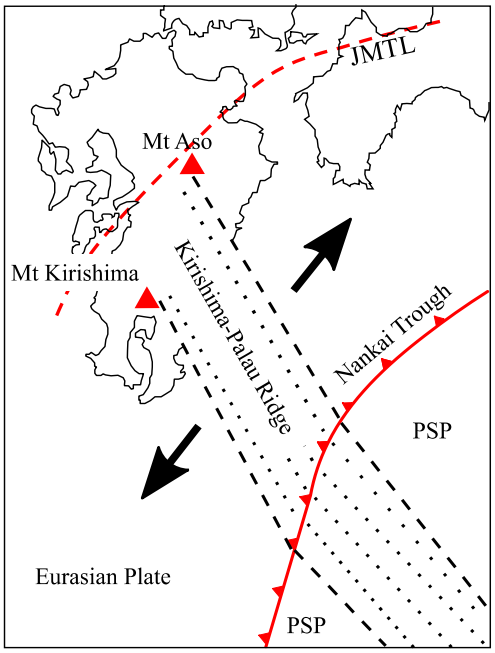

Figure 2: Tectonic map of South Kyushu at 10Ma (PSP = Philippine Sea Plate, JMTL = Japan Median Tectonic Line) (Modified from Shibata *et al.*, 2014).

2.2 Geological Setting

Quaternary volcanism created the Kirishima Volcanics; a 400km^3 NW-SE ellipse consisting of 20 volcanic cones (Aizawa *et al.*, 2013) located parallel to major extensional faulting (NEDO, 1997). Volcanic stratigraphy (Fig 3) of the Kirishima region can be divided into four main stages which represent multiple periods of volcanism; Kirishima Volcanics (L. Pleistocene – Present), Kakuto Andesites (E. Pleistocene), Kirishima Welded Tuffs (Pliocene – Pleistocene) and Hokusatsu Andesites (Miocene – Pliocene) (Taguchi & Hayashi, 1983). These volcanic units successively overlay each other upon the Paleocene Shimanto Group basement (NEDO, 1997). Eruption centres have progressively migrated

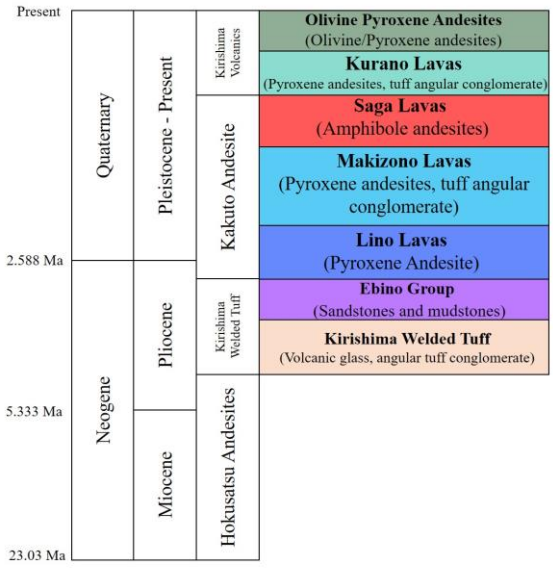

Figure 3: Stratigraphy of the Kirishima Volcanics (Modified from NEDO, 1997)

from the west to the east of the Kirishima Volcanics (Nagaoka and Okuno, 2011).

A key trend in the area is a series of normal faults orientated radially around the Kirishima Volcanics, although NW-SE faults are dominant with the Ebino area on the northern flanks. Faulting is found alongside thermal manifestations such as hot springs and fumaroles in addition to hydrothermally altered rock (Taguchi & Hayashi, 1983), indicating the relationship between the geothermal system and structural geology on the northern side of the Kirishima Volcanics. As a result of progressive volcanism, normal faulting led to the development of small NW-SE trending grabens which developed fractures in the Ogiri geothermal field (Sawaki *et al.*, 1997).

The geothermal reservoir (Fig 4) within the northern side of the Kirishima Volcanics is located in fracture zones in the Lino Group and Makizono lavas (Kakuto Andesites), whilst the Ebino Group and localised alteration act as sealing units (NEDO, 1997). Temperature data along the NW-SE trending Nagaegawa Fault, elevated between 216-220°C below 1400m (NEDO, 1997), shows the relationship between fluid and faulting, indicating that faults act as conduits for fluid flow and are responsible for the creation of fracture zones. A pressure gradient of 0.0625Kgf-cm^2/m was encountered when drilling along the east of the Nagaegawa Fault. Whilst faulting has created elevated temperature profiles, fluid inclusion analysis indicates the progressive cooling of the northern geothermal system compared to the western side of the Kirishima Volcanics; NW-SE faulting and minor NE-SW conjugate faulting have been associated with this cooling effect potentially due to the drawdown of shallow groundwater (Taguchi & Hayashi, 1983).

The origin of fluid within the geothermal system is from meteoric water infiltrating the Kirishima volcanic domes and becoming heated by contact with the Shimanto basement rock. Geothermal fluid subsequently rises through major

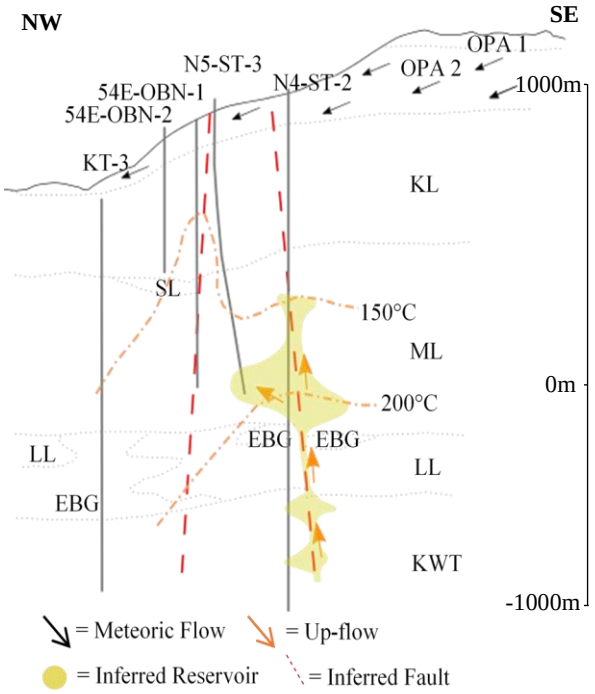

Figure 4: Geothermal system (Modified from NEDO, 1997)

NW-SE faults, creating an up-flow zone along the southwest margin of the Ebino area, and migrates towards the south where permeability is located in the fractured Makizono lava (NEDO, 1997).

3. EXPLORATION HISTORY

The frequency of volcanoes in the Kirishima Volcanics has subsequently produced frequent eruptive activity and associated surface manifestations such as fumaroles, predominantly from Iwo-yama, Ohachi, and Shinmoe-dake (Aizawa *et al*., 2013). Sustained volcanism, alongside the presence of multiple hot springs located to the north of the volcanic group in the Shiratori area, indicate the presence of subsurface geothermal activity. Early geothermal exploration was focused on the west and northern side of the Kirishima Volcanics, where Nitettsu Mining Company (NMC) carried out initial surface exploration in 1972 to collect gravity, resistivity, magnetics and surface temperature datasets (Garg *et al*., 1998). Subsurface exploration was carried out from 1975 to 1997 where a total of 42 boreholes were drilled by NEDO and the Nippon Steel Corporation (Hazama *et al.*, 1988). Exploration and subsequent reservoir simulations indicated that the Ginyu Fault, located to the north of the Kirishima Volcanics, was economically capable of producing a steam production equivalent of 35MW (Hazama *et al.*, 1988). In 1996 the Ginyu Fault was developed as part of the Ogiri geothermal field which targeted a fractured feed zone between 1100-1350m, featuring a uniform temperature of 232°C and a production capacity of 30MW (Goko, 2000).

NEDO concluded that geothermal development on the western margin of the Kirishima Volcanics was uneconomic due to energy market constraints and the efficiency of flash turbine generators however, due to changes in Japanese energy tariffs and advances in binary technology, the economic viability of development can be re-evaluated. Despite NEDO data confirming permeability at 1005m & 1225m (NEDO, 1997), further exploration is required to better understand the reservoir architecture and association with the surrounding structural geology. To achieve this, SE techniques are suited based on their high vertical resolution and integration with 3D modelling.

4. 3D MODELLING

4.1 Leapfrog 3D modelling software

Leapfrog is a 3D modeling software, created by ARANZ Geo, that enables the flexible integration of geological, structural, geophysical and reservoir data using implicit modeling methods (Alcaraz *et al*. 2011; McDowell and White, 2014). Rapid radial basis function (RBF) interpolation techniques promote flexibility by allowing models to be quickly created and modified as more data becomes available, providing a dynamic solution to geological visualization and interpretation.

4.2 Data

Datasets included in this model are as follows: topography derived from well collars, four major NW-SE trending faults, SE data, NEDO report well data including temperature, formations, feed zones (two in well N7-ST-6 from depths 1040.55 m to 1143.5 and 1277.37 m to 1359.72 m producing fluid at rates of 30.1 t/h and 18.9 t/h respectively), hydrothermal alteration zones, and NEDO report cross sections (two of which trend NW-SE and one trending NE-SW).

The model displays the volcanic stratigraphy within the survey area. All seven units thin to the north moving away from the volcanic centres located to the south of the Ebino area. The Saga lava thins and pinches out northwards against the Makizono lava below and Kurano lava above. The Ebino Group thins and pinches out southwards against the Lino Group below and Makizono lava above.

Temperature data from the NEDO wells are represented as isotherms in increments of 50°C. From 150°C, upwards, the isotherms are in increments of 10° C. The highest recorded temperature is 209.6°C in well KT-4.

SE data from recent geophysical surveying is grouped into three layers; upper (blue), middle (yellow), and lower (green). Data has been visualised to show the survey point locations alongside the top and bottom depths of the SE signal.

The model boundaries are constrained in the Z plane by the maximum depth of the deepest well drilled (KT-5), and in the XY plane by the spread of well collars in the Ebino survey area. The model is 2,400m x 2926m x 5434m (depth x width x length). The highest elevation in the area is 1,092m and the lowest elevation is 273m. The total volume of the model is ~38,000km^3.

4.3 Ebino geological model

Areas of high thermal activity vary within the Ebino model as a function of depth and location to faulting (Fig 5). At shallow depths of 0m above sea level (ASL) the 100°C isotherm is elevated in the centre of the model dominated by the geothermal gradient around well 54E-OBN-1; this anomaly is amplified until the 170°C isotherm. The 180°C isotherm shows a more homogenous temperature distribution compared to shallower isotherms, however shows localised thermal anomalies at three main locations trending NNE-SSW across the survey area. When fault zones are integrated with temperature data it is evident that thermal anomalies are located along each NW-SE fault, with steeper geothermal gradients being found on the most northern and southern faults. Whilst the highest geothermal gradient at shallow depths can still be found around 54E-OBN-1, the anomalies around KT-4 & N7-ST-6 are more laterally extensive and able to reach temperatures in excess of 200°C; this is shown by the elevated 200°C isotherm in the south of the area. However, it appears well temperatures may not have reached static reservoir temperatures as the shut-in time was only five days. Significant inversions are seen in KT-4 and N7-ST-6 which may need further evaluation to prove their existence.

The elevated temperatures associated with the faults suggests that faults, or fracture zones associated with the faults, are potential conduits for fluid flow from deep heated meteoric water charging fractured reservoir zones within the Lino Group and Makizono lava to the south and a shallower reservoir zone associated with well 54E-OBN-1 in the north. This shallow reservoir is located within the Saga lava and overlying Kurano lava, possibly capped by an alteration layer within the Kurano lava or the Olivine Pyroxene Andesite. Geothermal gradients still vary between each of the fault zones, which potentially provides an insight into the location of the upflow zone in addition to an understanding of the

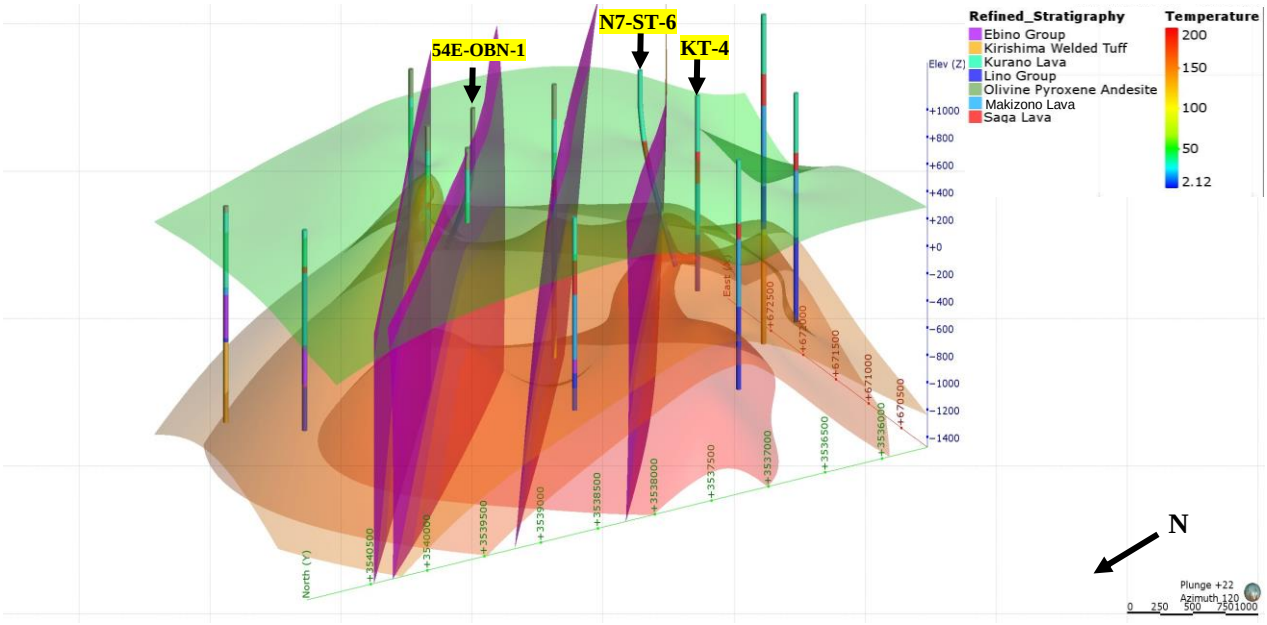

Figure 5: Ebino model showing isotherms, borehole geology & faulting.

permeability within each fault. Based on the 180°C and zones, which potentially provides an insight into the location of the upflow zone in addition to an understanding of the permeability within each fault. Based on the 180°C and 200°C isotherms, indications are that the most southern fault is proximal to the upflow zone and an effective conduit for the migration of heated fluids to shallower depths. Whilst the 200°C isotherm is predominant around well N7-ST-6, temperature inversion within the KT-4 well has subsequently created an anomalous isotherm lobe located perpendicular to the closest NW-SE fault (Fig 6). The temperature inversion associated with this fault in wells N7-ST-6 and KT-4 maybe due to a zone of high permeability, where a localised fracture zone close to faulting provides a conduit for hotter geothermal fluid to rise and circulate at shallower depths. Subsequently, static reservoir temperatures may not have stabilised due to the short shut-in period as mentioned above. Na/K (Fournier) and Na-K-Mg liquid geothermometry from N7-ST-6 suggests reservoir temperatures at 225°C and partial thermal equilibrium.

The distribution of alteration minerals varies across the survey area with noticeable differences between the north and south (Fig 7). Montmorillonite is dominant across the entire survey area and features the thickest alteration intervals in borehole data. Alkali feldspar alteration is found predominantly in the north of the survey area, close to 54E-OBN-1, from depths between 400m to -400m ASL. The presence of alkali feldspar, combined with elevated geothermal gradients at shallow depths, are concordant with shallow geothermal activity with hydrothermal fluid in excess of 170°C (Reyes, 1990). Silica alteration is focused around the southernmost fault between 400m to -100m ASL, above areas with elevated geothermal gradients. This may indicate

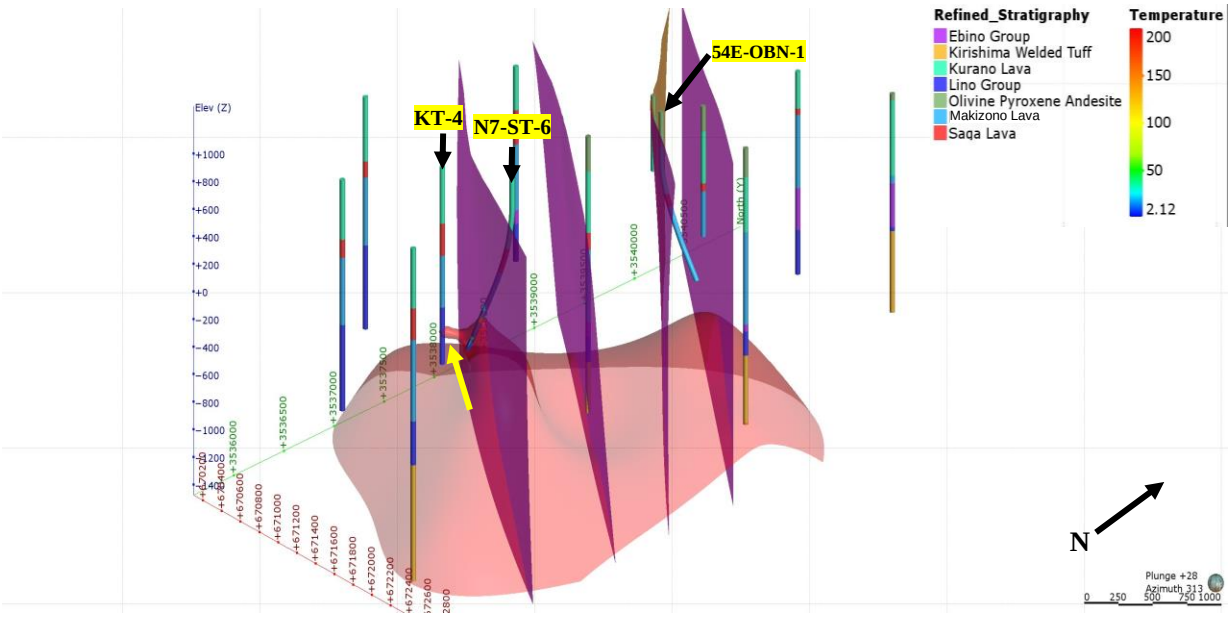

Figure 6: 200°C isotherm alongside borehole geological and NE-SW faulting. Inversion anomaly highlighted (arrow).

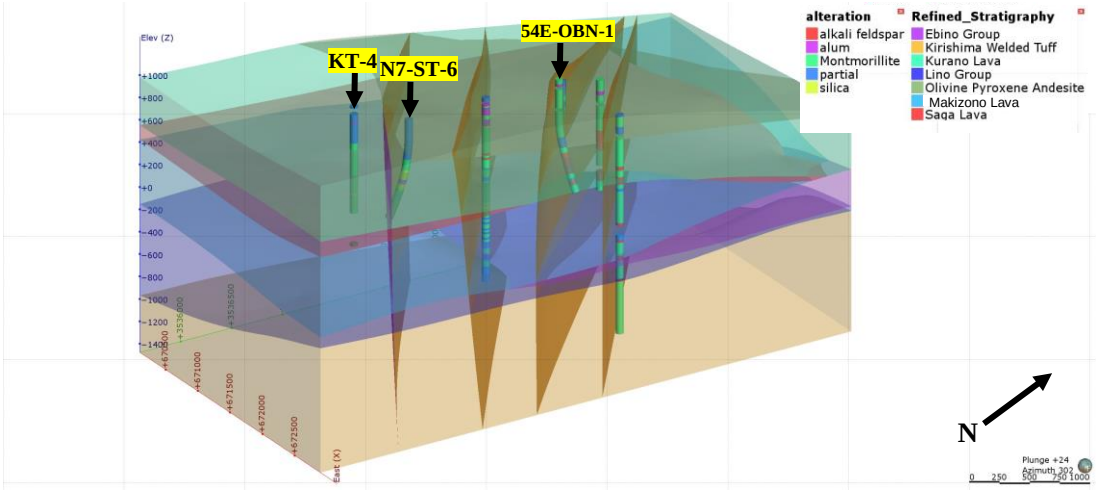

Figure 7: Distribution of borehole alteration minerals alongside 3D geological and structural data.

that these thin silica units are acting as a localised seal to inhibit the migration of geothermal fluid to shallower depths; variations in the 150°C and 100°C isotherms support this.

Geological and numerical data from previous exploration in the Ebino area have provided insights into the potential geothermal system; elevated isotherms are located close to NW-SE fault zones and suggest faulting acts as a conduit for fluid migration. Reservoir permeability is likely to be fractured zones within the Lino Group proximal to faulting, explaining the presence of isotherm anomalies, however their locations and laterally continuity away from boreholes remains unknown.

5. SEISMO-ELECTRIC DATA

5.1 Introduction

The Seismo-Electric (SE) effect is associated with charge activities taking place at the mineral-water interface, defined as the electrical double layer (EDL). Seismic waves pass through porous rocks and differentially agitate both the rock frame and the pore fluid at different speeds. Relative movement between the fluid and solid particles disturbs the EDL which in turn produces an electric charge (Revil *et al*., 2015). The variation in electric charge creates an electric potential signal, which can be detected at the surface as electrical signals.

SE applications are predominantly associated with groundwater (Butler *et al*., 2002; Dupuis *et al*., 2007), geotechnical (Skokan & Chi, 1993) and petroleum exploration (Hong, 1994; Revil & Jardani, 2010). The use of SE techniques for geothermal exploration remains low, as utilization is focused around monitoring hydraulic fracturing in enhanced geothermal systems (EGS) (Marquis *et* al., 2003; Warden *et al*., 2017).

SE is advantageous in challenging topographies due to its exclusively vertical sampling profile. This is suitable for the Ebino area that is divided by multiple valleys that trend NW-SE, making large sections inaccessible. These constraints reduce the horizontal area required for MT and gravity surveys. Data acquisition time for SE is low allowing prompt interpretations and future development planning compared to other geophysical surveying techniques. SE results need to be integrated with other geoscientific methods especially at greater depths to give context to the results.

5.2 Re-evaluated geological model

Three possible, permeable fluid-saturated zones are shown when SE data is incorporated into the existing geological model (Fig 8); an upper layer located within the Makizono lava and Saga lava, a middle layer within the Lino Group, and

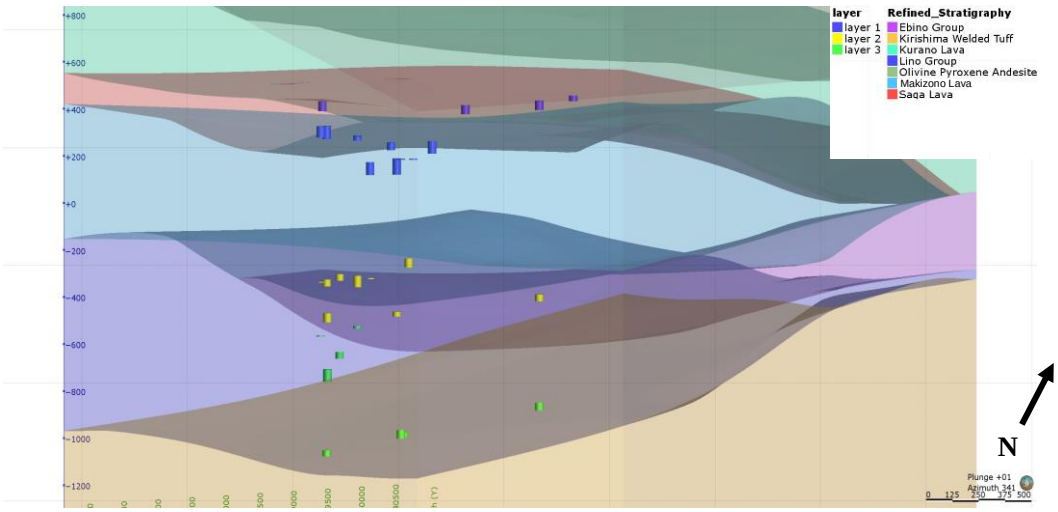

Figure 8: SE signals within geological model

lower layer located in the Kirishima Welded Tuff and Lino Group.

All SE signals were detected in proximity to the southernmost fault in the survey area, with a larger proportion of middle and lower signals derived from the southern footwall (Fig 9). SE

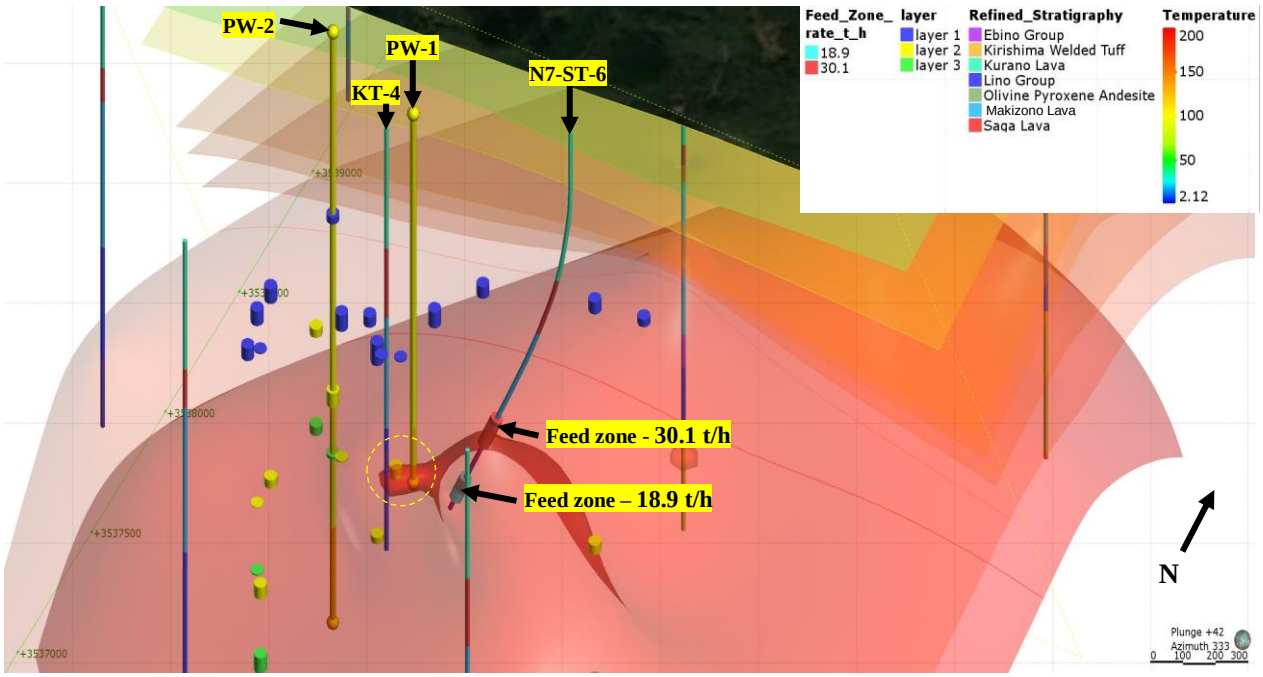

Figure 9: 38 m thick SE signal within temperature inversion zone (highlighted). Planned wells (PW) 1 and 2 with SE signals, feed zones, temperature isotherms and NEDO wells.

signals from the upper zone show the highest lateral continuity occurring across the southernmost faults and towards the southwest within a depth range of 120m. Upper zone data also features the thickest signal intervals, averaging 36m. Signal frequency and interval thickness in the middle and lower SE zones show a lack of lateral continuity.

SE data with temperature isotherms may give initial indications of the distribution of fracture zones along faults. A 38m thick SE signal is located between wells KT-4 & N7-ST-6, parallel to the 18.9t/h feed zone, within the temperature inversion at the 200°C isotherm. This evokes the possibility that a fluid saturated fracture zone, penetrated by well KT-4, exists on the hanging wall of the southernmost fault connecting the well bore to high temperature reservoir fluids. This also provides more context that may indicate well bore heat up surveys were not in equilibrium with the static reservoir. If this is the case it is possible that permeable high temperature reservoir may continue to the south.

Incorporating SE data into the existing geological model has led to the identification of potentially fluid saturated zones close to faulting which, when combined with temperature data, can assist in identifying high value drilling targets. Areas that contain multiple SE signals have been examined by planning wells to simulate expected geothermal temperature profiles. Results show that prospects are located in the southwest of the Ebino area, close to faulting and former exploration wells, expected to reach temperatures of 201°C at 1250 m and 209°C at 2000 m respectively (Fig 10). PW-1 productivity is expected to be analagous to the performance shown in the lower feed zone of N7-ST-6, and expected to be laterally continuous to the south as shown by KT-4 temperature data.

6. CONCLUSION

The integration of existing exploration data alongside SE survey results have updated the geothermal model for the Ebino area defined by NEDO exploration, reaffirming evidence for a potentially productive geothermal system.

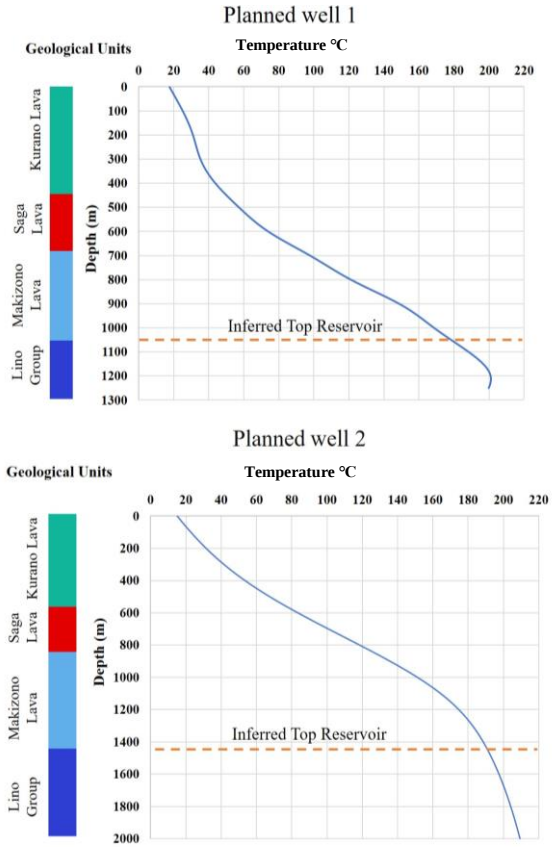

Figure 10: Temperature profile with depth and geological units for planned wells 1 (top) & 2 (bottom).

Integrated data suggests the Makizono formation may have the highest density of fractured zones which may be the most prolific for shallow production. Based on SE surveying and previous exploration data, two well prognosis examples have been tested in the model as examples for future drilling.

3D modeling has provided an effective solution for visualizing subsurface conditions using multiple datasets, where understanding of the geothermal activity in the Ebino area has been subsequently improved.

7. FURTHER WORK

As prospects within the Ebino area have been confirmed and verified through drilling and geophysical surveying, future steps will be to progress with the exploration campaign and plan boreholes (Fig 9) that will provide a better understanding of the reservoir fluid conditions & dynamics. Reservoir data will be simulated using TOUGH2 and visualized, having upscaled the current version of the static geological model.

ACKNOWLEDGEMENTS

We would like to thank Geothermal Development & Investment (GDI) for giving us permission to publish the data.

REFERENCES

Aizawa, K., Koyama, T., Uyeshima, M., Hase, H., Hashimoto, T., Kanda, W., Yoshimura, R., Utsugi, M., Ogawa, Y. and Yamazaki, K.I.: *Magnetotelluric and temperature monitoring after the 2011 sub-Plinian eruptions of Shinmoe-dake volcano*. Earth, Planets and Space, 65(6), pp. 6. (2013).

Alcaraz, S., Lane, R., Spragg, K., Milicich, S., Sepulveda, F. and Bignall, G.*: 3d geological modelling using new Leapfrog Geothermal soft-ware*. In Proceedings of 36th Workshop on Geo-thermal Reservoir Engineering, Stanford University, USA. January. (2011).

Butler, K.E., Kepic, A.W. and Rosid, M.S.: *An experimental seismoelectric survey for groundwater exploration in the Australian outback.* In SEG Technical Program Expanded Abstracts 2002. Society of Exploration Geophysicists. pp. 1484 - 1487. (2002).

Dupuis, J.C., Butler, K.E. and Kepic, A.W.: *Seismoelectric imaging of the vadose zone of a sand aquifer*. Geophysics, 72(6). pp. A81-A85. (2007).

Garg, S.K., Combs, J., Kodama, M. and Gokou, K.: *Analysis of production/injection data from slimholes and large-diameter wells at the Kirishima geothermal field, Japan.* In Proceedings, Twenty-Third Workshop on Geothermal Reservoir Engineering. pp. 26-28. (1998).

Goko, K.: *Structure and hydrology of the Ogiri field, West Kirishima geothermal area, Kyushu, Japan*. Geothermics, 29(2). pp.127 - 149. (2000).

Hazama, Y., Nagao, S., Abe, I., and Monden, Y.: *Reservoir Simulation on the Kirishima Geothermal Field*. Japan International Geothermal Symposium. pp. 140 - 143. (1988).

Hong, L.I.U.: *The Prospective Application of Seismo-Electric Effect in Natural Resources Exploration [J]*. Progress In Geophysics, 2. pp. 003. (2002).

International Finance Corporation (IFC): *Success of Geothermal Wells: A Global Study*, World Bank Group, pp. 18. (2013).

Kimura, G.: *Collision orogeny at arc-arc junctions in the Japanese islands: The Island Arc*. 5(3): pp. 262 – 275. (1996).

Marquis, G., Darnet, M., Michelet, S. and Baria, R.: December. *Observations of Seismoelectric Signals Induced by a Hydro-fracturing Experiment in a Deep Geothermal Reservoir*. *In* AGU Fall Meeting Abstracts. (2003).

McDowell, J. and White, P.: *Updated resource assessment and 3-D geological model of the Mita Geothermal System, Guatemala*. In Geothermal Resources Council 2011 Annual Meeting. pp. 99 - 107. (2011).

Miyoshi, M., Fukushima, T., Sano, T. and Hasenaku, T.: *Subduction influence of Philippine Sea plate on the mantle beneath northern Kyushu, S.W. Japan: an examination of boron contents in basaltic rocks*. J. Volc. Geotherm. Res., 171. pp. 73 - 87. (2008).

Nagaoka, S. and Okuno, M.: *Tephrochronology and eruptive history of Kirishima volcano in southern Japan*. Quaternary international, 246(1). pp. 260 - 269. (2011).

NEDO (New Energy and Industrial Technology Development Organisation): Geothermal Development Promotional Research Report No. C-1: Shiratori area. (1997).

Park, J.O., Hori, T. and Kaneda, Y.: *Seismotectonic implications of the Kyushu-Palau ridge subducting beneath the westernmost Nankai forearc*. Earth, planets and space, 61(8). pp. 1013 - 1018. (2009).

Revil, A., Jardani, A., Sava, P. and Haas, A.: *The Seismoelectric Method: Theory and Application*. John Wiley & Sons. (2015).

Revil, A. and Jardani, A.: *Seismoelectric response of heavy oil reservoirs: theory and numerical modelling*. Geophysical Journal International, 180(2), pp. 781 - 797. (2010).

Reyes, A.G.*: Petrology of Philippine geothermal systems and the application of alteration mineralogy to their assessment.* Journal of Volcanology and Geothermal Research, 43(1-4), pp. 279 - 309. (1990).

Sawaki, T., Sasada, M., Sasaki, M. and Goko, K.: *Fluid inclusion study of the Kirishima geothermal system, Japan*. Geothermics, 26(3), pp. 305 - 327. (1997).

Shibata, T., Yoshikawa, M., Ujike, O., Miyoshi, M. and Takemura, K.: *Along-arc geochemical variations in Quaternary magmas of northern Kyushu Island,*

Japan. Geological Society, London, Special Publications, 385(1), pp. 15 - 29. (2014).

Skokan, C.K. and Chi, D.: *LABORATORY INVESTIGATIONS OF THE SEISMO-ELECTRIC EFFFECT*. Subsurface Exploration Technology. pp. 425. (1993).

Taguchi, S. and Hayashi, M.: *Past and present subsurface thermal structures of the Kirishima geothermal area, Japan*. Geothermal Resources Council, Transactions, 7. pp. 199 - 203. (1983).

Warden, S., Sailhac, P. and Garambois, S.: *Microseismoelectric Monitoring-A New Technique to Monitor Hydraulic Stimulation Processes*. In 79th EAGE Conference and Exhibition 2017. June. (2017).

Watanabe, Y.: *Late Cenozoic evolution of epithermal gold metallogenic provinces in Kyushu, Japan*. Mineraliums Deposita, 40. pp. 307 - 323. (2005).